Earth and Environmental Science Transactions of the Royal Society of Edinburgh, **112**, 101–110, 2021

Article

Theoretical inversion of the fossil hydrothermal systems with oxygen isotopes of constituent minerals partially re-equilibrated with externally infiltrated fluids

Chun-Sheng WEI* and Zi-Fu ZHAO

CAS Key Laboratory of Crust-Mantle Materials and Environments, School of Earth and Space Sciences, University of Science and Technology of China, Hefei 230026, China.
*Corresponding author. Email: wchs@ustc.edu.cn

ABSTRACT: While the external infiltration of water has been identified from modern geothermal and/or fossil hydrothermal systems through stable isotopes, the physicochemical boundary conditions like the initial oxygen isotopes of water ($\delta^{18}O^{i}_{W}$) and rock as well as alteration temperature were implicitly presumed or empirically estimated by the conventional forward modelling. In terms of a novel procedure proposed to deal with partial re-equilibration of oxygen isotopes between constituent minerals and water, the externally infiltrated meteoric and magmatic water are theoretically inverted from the early Cretaceous post-collisional granitoid and intruded Triassic gneissic country rock across the Dabie orogen in central-eastern China. The meteoric water with a $\delta^{18}O^{i}_{W}$ value of −11.01 ‰ was externally infiltrated with a granitoid and thermodynamically re-equilibrated with rock-forming minerals at 140°C with a minimum water/rock $(W/R)_o$ ratio around 1.10 for an open system. The lifetime of this meteoric hydrothermal system is kinetically constrained less than 0.7 million years (Myr) via modelling of surface reaction oxygen exchange. A gneissic country rock, however, was externally infiltrated by a magmatic water with $\delta^{18}O^{i}_{W}$ value of 4.21 ‰ at 340°C with a $(W/R)_o$ ratio of 1.23, and this magmatic hydrothermal system could last no more than 12 thousand years (Kyr) to rapidly re-equilibrate with rock-forming minerals. Nevertheless, the external infiltration of water can be theoretically inverted with oxygen isotopes of re-equilibrated rock-forming minerals, and the ancient hydrothermal systems driven by magmatism or metamorphism within continental orogens worldwide can be reliably quantified.

KEY WORDS: central-eastern China, Dabie orogen, magmatic water, meteoric water.

During dynamic evolutions of the Earth, the interplays between the hydrosphere and lithosphere can considerably impact the mass and/or heat transfers, ore deposit formations, environmental changes, nuclear waste storage and/or disposal, life origin and/or extinction and much more (cf., extensive summaries therein by Henley *et al*. 1984; Walther & Wood 1986; Hochella & White 1990; Spencer & Chou 1990; Hellmann & Wood 2002; Oelkers & Schott 2009). Since the water–rock interaction is essentially triggered by natural heat engines, hydrothermal processes accompanying magmatism and/or metamorphism are more realistic for thermodynamic and kinetic considerations. Previous studies have documented the magmatism and/or metamorphism driven water–rock interactions worldwide (Taylor 1977; Taylor & O'Neil 1977; Nabelek *et al*. 1984; Wickham & Taylor 1985, 1987; Valley *et al*. 1986; Taylor *et al*. 1991; Wickham *et al*. 1993; Valley & Cole 2001; Holk *et al*. 2006; Holk & Taylor 2007). Because $^{18}O/^{16}O$ and $^{2}H/^{1}H$ ratios of meteoric water are usually far from equilibrium with most of common igneous rocks, a small influx of meteoric water could remarkably and/or effectively lower the oxygen and hydrogen isotopes of igneous rocks within continental settings. In this regard, much more efforts have been concentrated on the external infiltration of meteoric water with the continental igneous rock during past decades (Taylor 1971; Turi & Taylor 1971; Taylor & Forester 1979; Criss & Taylor 1986; Holt & Taylor 1998).

While diverse water–rock interactions were characterised through stable isotopes, there still exist uncertainties such as (1) forward modelling, which presumes initial isotopic compositions of water and rock as well as re-equilibration temperature, has been widely applied, but inverse modelling is less conducted; (2) the disequilibrium of oxygen isotopes between susceptible and resistant accessary minerals has been well recognised but the achievement of partial re-equilibration among constituent minerals is less constrained; (3) igneous rock externally infiltrated by meteoric water is well emphasised but external infiltration of other sourced water with metamorphic rock is less concerned.

It is well known that there are major sources of natural water with distinctive origin (i.e., meteoric, oceanic, magmatic and metamorphic water, Sheppard 1981, 1986) that could potentially interact with various rocks. As summarised in Table 1, a large span of water–rock interactions could occur with different combinations between water and rock. Among them, the interactions between meteoric water and igneous rock as well as magmatic water and metamorphic rock are certainly affiliated to the inventories of external water infiltration.

Compared with the sedimentary processes dominated by basinal settings, magmatism and/or metamorphism are important geological activities and ubiquitously developed within continental orogens all over the world. While continental deep subduction and collision can be petrogenetically archived by

 doi:10.1017/S1755691021000244

Table 1 Internal (I) vs. external (E) water interaction with rock

Content	Sedimentary rock	Igneous rock	Metamorphic rock
Meteoric water	I or E[1]	***E***[2]	E
Seawater	I or E[1]	E[3]	E[3]
Magmatic water	E	I	***E***[2]
Metamorphic water	E	E[4]	I

[1]For terrestrial sedimentary rock, infiltration by late meteoric water is referred to as either internal or external interaction with some uncertainties. However, infiltration of meteoric water with early marine sedimentary rock is definitely external. Infiltration of a late seawater with terrestrial sedimentary rock is certainly external whereas its infiltration with early marine sedimentary rock is either internal or external.
[2]These infiltrations of external water with rock are theoretically inverted in this study.
[3]Tectonically, the continent–continent collision between the North and South China Blocks for the Dabie orogen was Triassic; there was no seawater thereafter to infiltrate with the high-temperature continental rocks.
[4]Due to an over 100 Ma gap between the Triassic metamorphism and the early Cretaceous post-collisional magmatism in the Dabie orogen, it is geochronologically less likely that the early metamorphic water was externally infiltrated with late igneous rocks.

magmatic and metamorphic rocks through source tracing, age dating and temperature calculating, the late fluid evolution of continental orogen was not sufficiently constrained up to now. Being one of the integrated components of continental orogen, the externally infiltrated fossil hydrothermal system accompanying magmatism and/or metamorphism could fill this gap and advance our understanding of the thermal history of continental orogen. Therefore, the early Cretaceous post-collisional granitoids and intruded Triassic gneissic country rocks across the Dabie orogen in central-eastern China were studied as natural examples because some of them were evidently infiltrated by external water and partially re-equilibrated for oxygen isotopes among constituent minerals.

1. Geological settings and their geochemical characters

The Dabie-Sulu orogen is characterised by the largest occurrence of microdiamond- and/or coesite-bearing ultrahigh pressure (UHP) metamorphic rocks in the world (Wang *et al*. 1989; Xu *et al*. 1992; Ye *et al*. 2000; Zheng *et al*. 2003; Zheng 2012). Triassic ages of 200 to 240 Ma were dated with different kinds of geochronometer for the eclogite-facies rocks and their cooling histories during exhumed processes were accordingly constrained (Li *et al*. 1993, 2000; Ames *et al*. 1996; Rowley *et al*. 1997; Hacker *et al*. 1998, 2000; Liu *et al*. 2006; Cheng *et al*. 2011). Furthermore, the world record ultrahigh $\varepsilon_{Nd}(t)$ value up to +264 was measured for eclogites (Jahn *et al*. 1996) and zircons with the lowest ever reported $\delta^{18}O$ values down to about −11 ‰ were found (Rumble *et al*. 2002; Zheng *et al*. 2004; Fu *et al*. 2013).

In contrast to the sporadically outcropped lenses or blocks of UHP eclogites, composite plutons and batholiths of the early Cretaceous post-collisional granitoid are the predominant igneous rocks, although a number of coeval small mafic to ultramafic plutons have been documented in the Dabie orogen (Xue *et al*. 1997; Ma *et al*. 1998; Jahn *et al*. 1999; Zhang *et al*. 2002; Bryant *et al*. 2004; Zhao *et al*. 2004, 2005, 2007, 2011; Xu *et al*. 2005; Wang *et al*. 2007; Xu *et al*. 2012; He *et al*. 2013; Deng *et al*. 2014; Dai *et al*. 2015). The early Cretaceous ages ranging from 125 to 135 Ma were dated for most of the plutons and batholiths using zircon U-Pb techniques. The upper intercept ages of Neoproterozoic for available zircon U-Pb dating indicated their affinities with the South China Block. Zircon Hf and whole-rock Nd-Sr isotopes suggested an old enriched source(s) was petrogenetically linked to the early Cretaceous post-collisional igneous rocks.

2. Sampling and analysing

The studied granitoids and their gneissic country rocks mainly occupy the northern and central-eastern lithotectonic units of the Dabie Block (DBB). From north to south, the Hepeng pluton (HP) outcrops in the utmost eastern tip of the Northern Huaiyang volcanic-sedimentary belt, whereas the Tianzhushan pluton (TZS) is adjacent to the Central Dabie UHP metamorphic belt (Fig. 1). The intrusive contact between granitoids and gneissic country rocks was unambiguously observed in the field. For comparison, two gneisses from the Sidaohe without being intruded by granitoids in the Hong'an Block were also studied.

Fresh medium-grained granitoids and gneisses were collected from quarries and/or along road cuttings. Petrographically, quartz, alkali feldspar, biotite and sometimes amphibole are major rock-forming minerals, and accessory minerals include zircon and magnetite.

Conventional crushing, gravimetric, heavy liquid and magnetic techniques were applied to separate and concentrate zircon, quartz and alkali feldspar from whole rocks. In order to avoid metamict zircons and other impurities, the separated zircons were sequentially treated with concentrated HCl, HNO_3 and HF acids under room conditions overnight. The purity of treated mineral separates is generally better than 98 % with optical microscope examination.

Oxygen isotopes were analysed with laser fluorination online techniques (Valley *et al*. 1995; Wei *et al*. 2008), and an airlock chamber was employed to avoid the 'cross-talk' of reactive alkali feldspar (Spicuzza *et al*. 1998). The conventional $\delta^{18}O$ notation in per mil (‰) relative to Vienna Standard Mean Ocean Water (VSMOW) is reported in supplementary Table 1 available at https://doi.org/10.1017/S1755691021000244.

In order to control the quality of $\delta^{18}O$ analysis, the garnet standard, UWG-2, was routinely analysed. For 15 analytical days over 3 months, the daily average of measured $\delta^{18}O$ values of UWG-2 varied from 5.54 to 5.89 ‰, and the daily analytical precision is better than ±0.11 ‰ (one standard deviation, 1 SD). Raw $\delta^{18}O$ values of mineral separates were accordingly corrected in terms of the accepted UWG-2 value of 5.80 ‰. The international standard, NBS 28 quartz, was analysed and the corrected $\delta^{18}O$ values for NBS 28 are from 9.31 to 9.69 ‰ during the course of this study.

The reproducibility of fresh crystalline zircon $\delta^{18}O$ analysis is excellent throughout this study. As shown in supplementary Table 1, the 1 SD of most duplicate measurements with one triplicate is less than ±0.10 ‰, which is within the maximum routine analytical uncertainties demonstrated by daily UWG-2 garnet standard measurements.

3. Results

As shown in supplementary Table 1 and Fig. 2, zircon $\delta^{18}O$ values of the gneisses scatter from −3.78 to 0.33 ‰, whereas zircon values of granitoids cluster around 5.16 ± 0.38 ‰ (1 SD, $n = 25$) and somehow overlap with mantle zircon. This suggests that the granitoids with uniform zircon $\delta^{18}O$ values cannot petrogenetically link to those heterogeneous gneisses, which are almost threefold larger than zircon $\delta^{18}O$ variability of the granitoids (4.11 vs. 1.42 ‰).

Some alkali feldspar $\delta^{18}O$ values of the granitoids, however, steeply shift down to low values and evidently depart from isotherms (Fig. 2a), indicating infiltration by low $\delta^{18}O$ water under post-magmatic conditions. While magmatic equilibrium fractionations are well preserved by most of the available zircon

https://doi.org/10.1017/S1755691021000244 Published online by Cambridge University Press

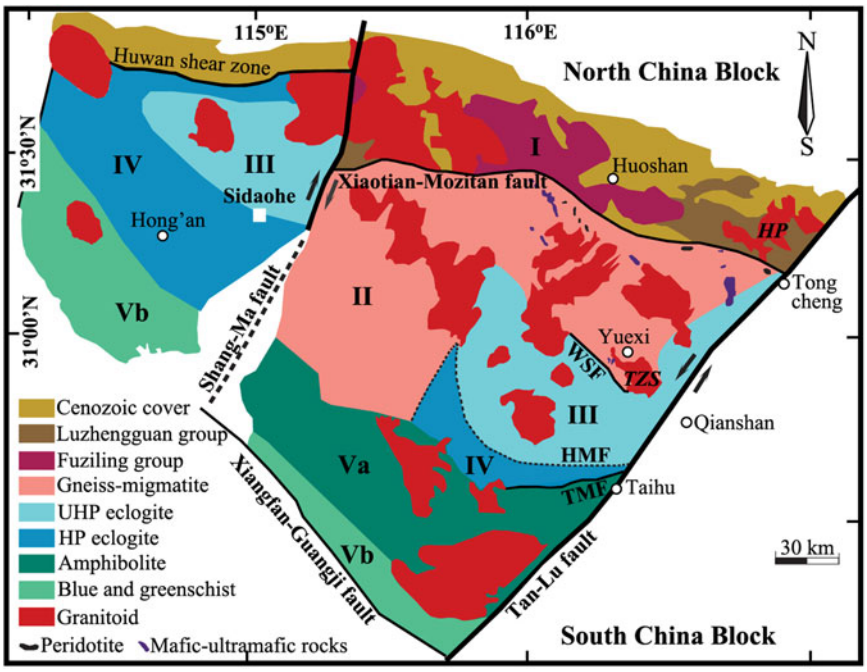

Figure 1 Geological sketch of the Dabie orogen modified from Ma *et al.* (1998), Zhang *et al.* (2002) and Ernst *et al.* (2007). In terms of field relation and lithological assemblage, geological units bounded with faults were divided. Traditionally, the western portion beyond the Shang-Ma fault was termed Hong'an (or Xinxian) Block. The DBB was bounded by the Shang-Ma fault in the west and the Tan-Lu fault in the east. From north to south, the DBB was further subdivided into five belts: I. the Northern Huaiyang volcanic-sedimentary belt (flysch series); II. the Northern Dabie ultrahigh temperature gneissic and migmatitic belt; III. the Central Dabie UHP metamorphic belt; IV. the Southern-central Dabie high pressure metamorphic belt; and V. the Southern Dabie intermediate- to low-grade metamorphic belt. Bold italic capital letters denote the abbreviations of studied plutons, other details refer to supplementary Table 1. WSF = Wuhe-Shuihou fault; HMF = Hualiangting-Mituo fault; TMF = Taihua-Mamiao fault, respectively.

and quartz oxygen isotopes for the granitoids (Fig. 2b), further checks show that quartz oxygen isotopes were somehow lowered for sample 01HP05 from the Hepeng pluton and a disequilibrium with zircon accordingly occurred.

In contrast, the alkali feldspar and quartz oxygen isotopes were concurrently elevated for a gneissic country rock from the Tianzhushan pluton (labelled sample 01TZS05 in Fig. 2). This suggests that they were infiltrated by high $\delta^{18}O$ water, and disequilibria with zircon were therefore resulted in. Another gneissic country rock from the same pluton, however, still retained equilibrium oxygen isotope fractionation between zircon and quartz (Fig. 2b), and accordingly yielded about 600°C of equilibrium temperature (Teq). Because this temperature is within the ranges from 585 to 655°C for the two gneisses which did not subsequently experience water disturbance from the Sidaohe, it is thus of geological significance and is applied to constrain the initial quartz and alkali feldspar $\delta^{18}O$ values in the course of theoretical inversion of external water infiltration with gneissic country rock.

4. Discussion

Because the oxygen diffusivity of zircon is considerably slower than that of quartz and alkali feldspar within hydrothermal systems (Giletti *et al.* 1978; Giletti & Yund 1984; Fortier & Giletti 1989; Watson & Cherniak 1997; Zheng & Fu 1998), zircon is thus one of the most resistant accessory minerals to subsequent water disturbance and can maintain its original $\delta^{18}O$ value well (Valley 2003; Wei *et al.* 2008). Disequilibria of oxygen isotopes therefore occur between the resistant and susceptible minerals during short-lived hydrothermal processes (Fig. 2), in good agreement with their kinetic behaviours. Since the discrepancy of oxygen exchange rates between quartz and alkali feldspar with water is less pronounced (Cole *et al.* 1983, 1992), re-equilibrations of rock-forming minerals were thus achieved for labelled samples during external water infiltrations (Figs 3–5). These make the following discussions possible and practicable.

5. Forward and inverse modellings of the external infiltration of water

5.1. Non-unique constraint with the conventional forward modelling

The water–rock interaction was previously formulated for forward modelling with oxygen isotopes in terms of mass balance (Taylor 1977). For a closed system, the following relationship is satisfied:

$$\left(\frac{W}{R}\right)_c = \left[\frac{\delta^{18}O_R^f - \delta^{18}O_R^i}{\delta^{18}O_W^i - (\delta^{18}O_R^f - \Delta^{18}O_W^R)}\right] \Big/ \left[\frac{n_W^O}{n_R^O}\right] \quad (1)$$

And for an open-system, a simplified relationship is then held:

$$\left(\frac{W}{R}\right)_o = \ln\left[\left(\frac{W}{R}\right)_c \cdot \left(\frac{n_W^O}{n_R^O}\right) + 1\right] \Big/ \left[\frac{n_W^O}{n_R^O}\right] \quad (2)$$

where W/R denotes the time-integrated water/rock ratio for a closed or open system. $\delta^{18}O$ values with subscript W or R denote water and rock, and superscripts i and f denote initial and final oxygen isotopes of water or rock prior to and after water–rock interactions, respectively. $\Delta^{18}O_W^R$ denotes oxygen isotope fractionation between rock and water, and n_W^O/n_R^O denotes the ratio of exchangeable oxygen content between water and rock.

Since most of the forward modellings for water–rock interaction were actually carried out for constituent minerals instead of whole rocks, the subscript R of $\delta^{18}O$ values was accordingly replaced for an indicated mineral in Eqs 1 and 2. On the other hand, except for the observed final oxygen isotopes for a specified mineral (i.e., $\delta^{18}O^f$ value) and corresponding n_W^O/n_R^O ratio, there are still three unknown variables to be solved. Among them, the $\delta^{18}O^i$ values of constituent minerals prior to water–rock interaction can be confidently constrained in most cases. However, the $\delta^{18}O_W^i$ and $\Delta^{18}O$ values (the latter is temperature dependent)

https://doi.org/10.1017/S1755691021000244 Published online by Cambridge University Press

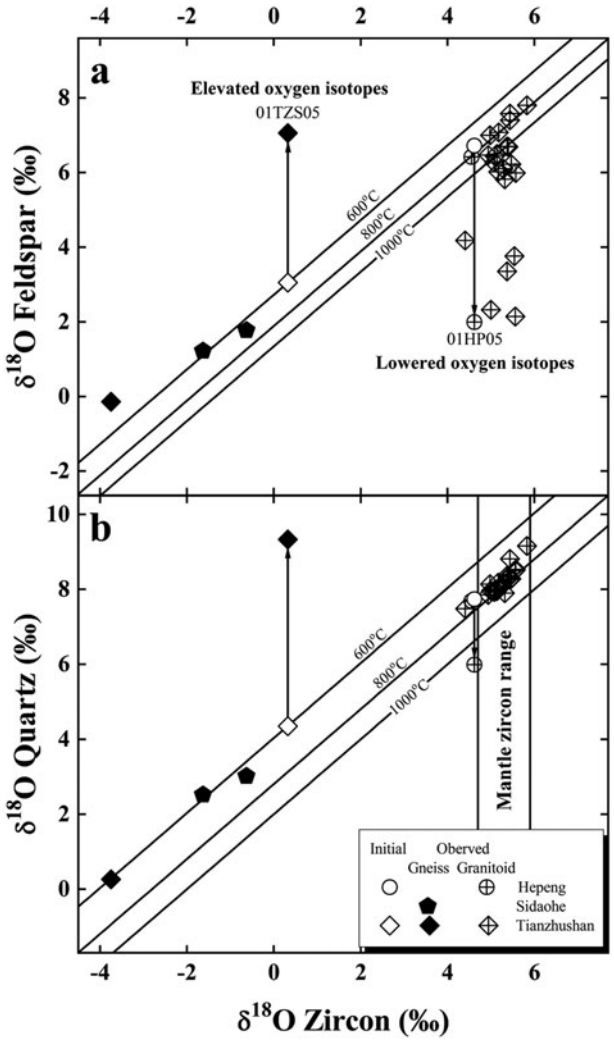

Figure 2 Diagrams of zircon vs. alkali feldspar (a) and quartz $\delta^{18}O$ values (b) for the granitoids and gneisses from Dabie orogen. Lines labelled with temperatures are isotherms after Zheng (1993), and two vertical lines in (b) denote the mantle zircon $\delta^{18}O$ value for comparison (Valley *et al*. 1998). Arrowed lines denote the disequilibrated oxygen isotopes theoretically inverted in this study. The observed and initial $\delta^{18}O$ values of constituent minerals refer to supplementary Tables 1 and 2, and the error bar is smaller than the symbol size throughout this study.

are usually empirically assumed or estimated through a trial and error procedure during the forward modelling of water–rock interaction. In other words, the $\delta^{18}O^{i}_{W}$ and $\Delta^{18}O$ values were first assumed in order to fit the observed $\delta^{18}O^{f}$ value. When the observed $\delta^{18}O^{f}$ value was mathematically matched, the $\delta^{18}O^{i}_{W}$ and $\Delta^{18}O$ values were then estimated. In principle, the two unknown variables of the $\delta^{18}O^{i}_{W}$ and $\Delta^{18}O$ values cannot be uniquely and/or simultaneously constrained with one observed $\delta^{18}O^{f}$ value by conventional forward modelling as shown below.

Because alkali feldspar and quartz oxygen isotopes were lowered together and departed from isotherms for sample 01HP05 from the Hepeng granitoid pluton (Fig. 2), it could be externally infiltrated by low $\delta^{18}O$ meteoric or oceanic water. Tectonically, the continent–continent collision between the North and South China Blocks for the Dabie orogen was Triassic (see section 1); there was no seawater thereafter to infiltrate with high-temperature continental rocks. Therefore, the concurrently lowered alkali feldspar and quartz oxygen isotopes and disequilibria with zircon observed for sample 01HP05 were ascribed to external infiltration by meteoric water, in good agreement with the following forward and inverse modellings.

Based on Eqs 1, 2 and parameters listed in Table 2, forward modelling is carried out to reproduce the observed $\delta^{18}O$ values for sample 01HP05. Two end-member situations are considered, i.e., external infiltration by meteoric water under an isothermal and constant $\delta^{18}O^{i}_{W}$ conditions, respectively.

Under an isothermal condition of 140°C retrieved from the oxygen isotopes of a quartz–alkali feldspar pair for sample 01HP05 (Table 2), the upper limit of $\delta^{18}O^{i}_{W}$ values is estimated to be about −10.40 ‰ from the observed alkali feldspar $\delta^{18}O$ value for a closed system with a very high $(W/R)_c$ ratio (labelled light solid curve in Fig. 3a). With the decrease in $\delta^{18}O^{i}_{W}$ to an extreme value of −20 ‰ for mid-latitude meteoric water, the $(W/R)_o$ ratio is systematically decreased to 0.21 for an open system (arrowed vertical light dashed line in Fig. 3a). Similar results obtain from the observed quartz $\delta^{18}O$ value although the upper limit of $\delta^{18}O^{i}_{W}$ values for meteoric water is estimated to be a slightly low value around −10.70 ‰ (labelled light solid curve in Fig. 3b), and the $(W/R)_o$ ratio decreases to 0.10 accompanied by a decrease in the $\delta^{18}O^{i}_{W}$ value of meteoric water (arrowed vertical light dashed line in Fig. 3b), respectively.

With the constant $\delta^{18}O^{i}_{W}$ value of −11.01 ‰ for meteoric water theoretically inverted from sample 01HP05 (Table 2), the lower limit of the re-equilibration temperature is estimated as *ca.*130°C from the observed alkali feldspar $\delta^{18}O$ value for a closed system (labelled light solid curve in Fig. 3c). With the re-equilibration temperature approaching the magmatic temperature of 740°C as the upper limit, the $(W/R)_o$ ratio is systematically decreased to 0.16 for an open system (arrowed vertical light dashed line in Fig. 3c). Forward modelling with the observed quartz $\delta^{18}O$ value also yields similar results. A slightly high lower limit of re-equilibration temperature is estimated as about 135°C for a closed system (labelled light solid curve in Fig. 3d), whereas the $(W/R)_o$ ratio is systematically decreased to an extremely low value of around 0.06 for an open system along with an increase in re-equilibration temperature (arrowed vertical light dashed line in Fig. 3d).

From the above discussions, it has been shown that forward modelling can only loosely estimate the upper limit of the $\delta^{18}O^{i}_{W}$ value and lower limit of re-equilibration temperature for external infiltration of meteoric water. The observed $\delta^{18}O$ values of different constituent minerals can be arbitrarily reproduced with noticeably varied $\delta^{18}O^{i}_{W}$ values ranging from −20 to −10.40 ‰, re-equilibration temperatures from 130 to 740°C and W/R ratios from 0.06 up to 110 through forward modelling. In other words, a unique solution cannot be obtained by conventional forward modelling. On the contrary, the external infiltration of unique meteoric water is theoretically inverted from sample 01HP05 (heavy curves in Fig. 3 and dashed curve with ticks in Fig. 4a, respectively).

5.2. The unique constraint with theoretical inversion

For constituent minerals thermodynamically re-equilibrated with water, the $\delta^{18}O^{i}_{W}$ value and W/R ratio can be uniquely and robustly inverted (Wei & Zhao 2017). For a closed system, equations were derived for alkali feldspar (Ksp) and quartz (Qtz), respectively:

$$\delta^{18}O^{f}_{Ksp}=\frac{\delta^{18}O^{i}_{Ksp}+[\delta^{18}O^{i}_{W}+(\Delta^{18}O^{Ksp}_{W})_r]\cdot(W/R)_c\cdot(n^{O}_{W}/n^{O}_{Ksp})}{1+(W/R)_c\cdot(n^{O}_{W}/n^{O}_{Ksp})} \quad (3)$$

$$\delta^{18}O^{f}_{Qtz}=\frac{\delta^{18}O^{i}_{Qtz}+[\delta^{18}O^{i}_{W}+(\Delta^{18}O^{Qtz}_{W})_r]\cdot(W/R)_c\cdot(n^{O}_{W}/n^{O}_{Qtz})}{1+(W/R)_c\cdot(n^{O}_{W}/n^{O}_{Qtz})} \quad (4)$$

https://doi.org/10.1017/S1755691021000244 Published online by Cambridge University Press

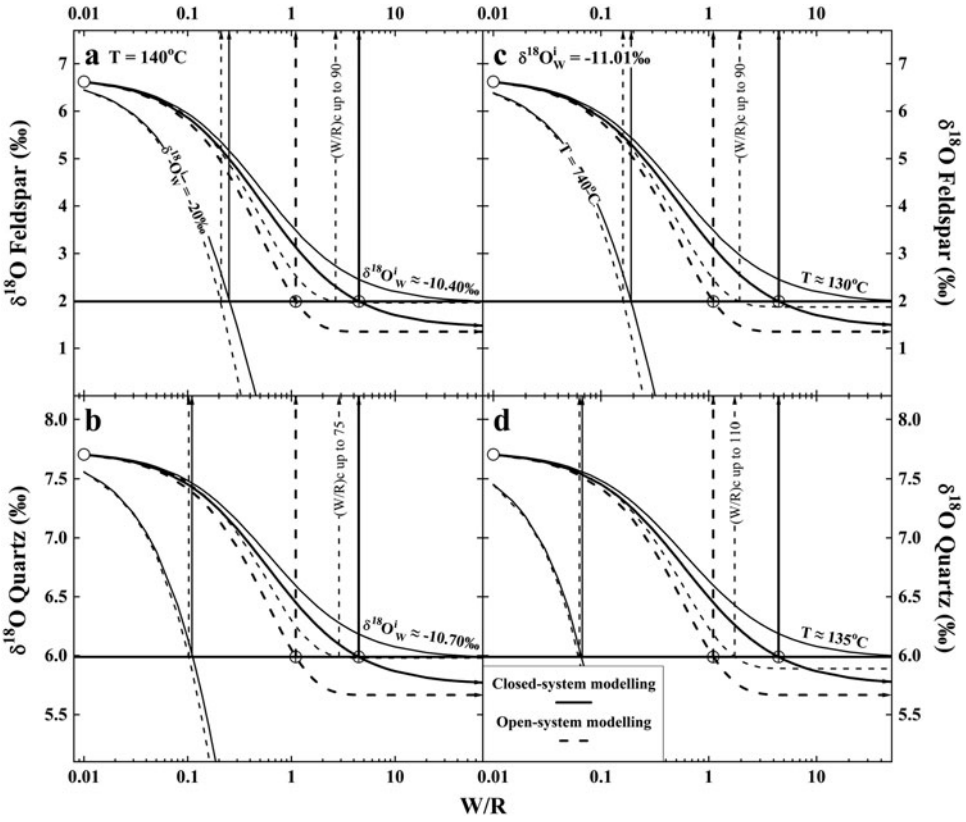

Figure 3 The external infiltration of meteoric water with granitoid from the Hepeng pluton (sample 01HP05). (a) and (b) denote trajectories of alkali feldspar and quartz $\delta^{18}O$ values along with W/R ratios, respectively, under an isothermal condition with varied $\delta^{18}O^{i}_{W}$ values. (c) and (d) denote trajectories under a condition of constant $\delta^{18}O^{i}_{W}$ value with varied temperatures. Symbol points connected by horizontal solid line illustrate the observed $\delta^{18}O$ values of rock-forming minerals from supplementary Table 1, whereas their initial values refer to Table 2. Arrowed vertical lines denote W/R ratios required to reproduce the observed $\delta^{18}O$ values, note that log10 scale of X axes is adopted for clarity.

and

$$\delta^{18}O^{i}_{Ksp}=\delta^{18}O^{i}_{Zrc}+(\Delta^{18}O^{Ksp}_{Zrc})_{m}\ \text{or}\ \delta^{18}O^{i}_{Qtz}=\delta^{18}O^{i}_{Zrc}+(\Delta^{18}O^{Qtz}_{Zrc})_{m} \quad (5)$$

Among all of the variables in Eqs 3–5, $\delta^{18}O^{f}_{Ksp}$ and $\delta^{18}O^{f}_{Qtz}$ are final values observed for a specified mineral; $\delta^{18}O^{i}_{Ksp}$ and- $\delta^{18}O^{i}_{Qtz}$ values can be calculated by Eq. 5 with the observed zircon (Zrc) $\delta^{18}O$ value at magmatic or metamorphic temperature (i. e., $(\Delta^{18}O^{Ksp}_{Zrc})_{m}$ or $(\Delta^{18}O^{Qtz}_{Zrc})_{m}$ value); and $(\Delta^{18}O^{Ksp}_{W})_{r}$ or $(\Delta^{18}O^{Qtz}_{W})_{r}$ value can be calculated with the re-equilibration temperature. Moreover, n^{O}_{W}/n^{O}_{Ksp} and n^{O}_{W}/n^{O}_{Qtz} ratios are actually constants between water and alkali feldspar as well as quartz (last row in Table 2). In this case, both the $\delta^{18}O^{i}_{W}$ value and the $(W/R)_{c}$ ratio can thus be solved out by combining Eqs 3 and 4.

In order to be self-consistent, theoretically calculated oxygen isotope fractionations are adopted throughout this study (Zheng 1993). Because the discrepancy between theoretical calculation and experimental calibration or empirical estimation is not notable for oxygen isotope fractionations of the studied constituent minerals, this will not significantly influence our results.

For an open-system, a similar inverse procedure can be applied. Owing to the natural logarithm (i.e., ln term in Eq. 2) or exponential function, an analytical expression cannot be obtained. Under this circumstance, a numerical reiteration with precision of at least 0.0001 is conducted to theoretically invert the $\delta^{18}O^{i}_{W}$ value and $(W/R)_{o}$ ratio.

5.2.1. Meteoric water with a low $\delta^{18}O^{i}_{W}$ value theoretically inverted from granitoid. As shown in Table 2 and Figs 3, 4a, oxygen isotopes of quartz were re-equilibrated with alkali feldspar at 140°C for sample 01HP05 from the Hepeng granitoid pluton. In terms of Eqs 3–5, the $\delta^{18}O^{i}_{W}$ value is theoretically inverted as −11.01 ‰ for an open system. It is certain that it was an externally infiltrated meteoric water.

On the basis of parameters listed in Table 2, the lowered oxygen isotopes of rock-forming minerals are well reproduced (Figs 3, 4a). A minimum $(W/R)_{o}$ ratio of 1.10 is accordingly quantified. It is worth pointing out that a systematically high $(W/R)_{c}$ ratio is required if a closed system is adopted (arrowed heavy-solid vs. -dashed vertical lines in Fig. 3).

The external infiltration of cold meteoric water not only lowered the oxygen isotopes of the granitoid but also thermally enhanced its cooling. This is in good agreement with the low re-equilibration temperature of 140°C retrieved from sample 01HP05 in Table 2. Furthermore, this low re-equilibration temperature temporally implied that meteoric water was externally infiltrated during the post-magmatic stage and/or spatially localised within the upper portion of the granitoid pluton, which is geologically consistent with the high-level emplacement within the upper crust of the Northern Huaiyang volcanic-sedimentary belt (Fig. 1).

5.2.2. Magmatic water with a moderately high $\delta^{18}O^{i}_{W}$ value theoretically inverted from gneissic country rock. For sample 01TZS05 from the gneissic country rock intruded by the Tianzhushan granitoid pluton, both alkali feldspar and quartz oxygen isotopes were evidently elevated and departed from the isotherms (Fig. 2). Hence, these observed disequilibria with zircon oxygen isotopes could be overprinted by high $\delta^{18}O$ water.

Given that quartz oxygen isotopes were re-equilibrated with alkali feldspar at 340°C (Table 2; Fig. 4b), the $\delta^{18}O^{i}_{W}$ value is theoretically inverted as 4.21 ‰ for an open system. The elevated oxygen isotopes of rock-forming minerals are satisfactorily reproduced (Fig. 4b, supplementary Fig. 1), and a minimum $(W/R)_{o}$ ratio of 1.23 is thus calculated.

https://doi.org/10.1017/S1755691021000244 Published online by Cambridge University Press

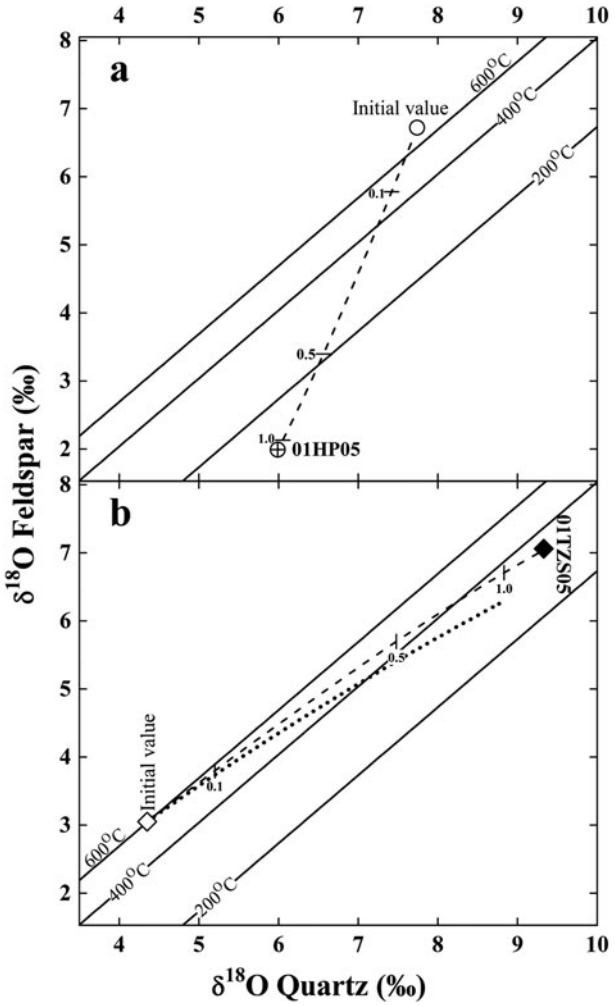

Figure 4 Diagrams of quartz vs. alkali feldspar $\delta^{18}O$ values for the granitoid (a) and gneissic country rock (b). Dashed curves denote the trajectories of rock-forming mineral $\delta^{18}O$ values infiltrated by the external meteoric or magmatic water theoretically inverted in Table 2, respectively, for open systems. Small ticks with numbers are $(W/R)_o$ ratios. The dotted curve in (b) demonstrates forward modelling with the internally buffered metamorphic water, calculated with the observed zircon $\delta^{18}O$ value at 600°C for sample 01TZS05.

The $\delta^{18}O^i_W$ value of 4.21 ‰ somehow overlaps with that of either metamorphic or magmatic water (cf., Sheppard 1986). Forward modelling with an internally buffered metamorphic water during the exhumed process, however, is too low to reproduce the observed $\delta^{18}O$ values (dotted curve in Fig. 4b). Therefore, elevated oxygen isotopes of sample 01TZS05 were externally infiltrated by magmatic water. This is geochronologically consistent with the available zircon U-Pb dating result (Zhao *et al*. 2008), that is, the studied Triassic gneissic country rock was subsequently superimposed by the early Cretaceous post-collisional magmatism of the adjacent Tianzhushan granitoid pluton. On the other hand, the moderately high $\delta^{18}O^i_W$ value of 4.21 ‰ could be the result of binary mixing between magmatic and meteoric water prior to external infiltration with gneissic country rock (Wei & Zhao 2017).

In contrast to external infiltration of cold meteoric water discussed in section 5.2.1., gneissic country rock was thermally re-equilibrated at 340°C with external infiltration of hot magmatic water for sample 01TZS05 (Table 2). This mildly warm re-equilibration temperature geologically suggests that the more deeply buried Triassic gneissic country rock was externally infiltrated by early Cretaceous magmatic water at least within the middle crustal settings, where the re-equilibration of oxygen isotopes between rock-forming minerals and magmatic water was kinetically facilitated (see section 7).

6. The reliability of $\delta^{18}O^i_W$ values

In order to theoretically invert $\delta^{18}O^i_W$ values, initial $\delta^{18}O$ values of rock-forming minerals and re-equilibration temperature are prerequisites (Wei & Zhao 2017 and Eqs 3–5 in section 5.2). The initial $\delta^{18}O$ values of rock-forming minerals prior to external water infiltration are calculated with the observed zircon oxygen isotopes at magmatic or metamorphic temperatures (Eq. 5), whereas the re-equilibration temperatures are calculated with the observed $\delta^{18}O$ values of quartz–alkali feldspar pairs for corresponding samples (Table 2). In these aspects, the validity of $\delta^{18}O^i_W$ values is evaluated as below.

It can be seen that $\delta^{18}O^i_W$ values of meteoric water theoretically inverted from the granitoid are gradually increased and converged when magmatic temperatures are increased from 500 to 850°C for sample 01HP05 (Fig. 5a). Moreover, subtle increase of $\delta^{18}O^i_W$ values is systematically inverted for the closed system all over the adopted temperature range (solid vs. dashed curve in Fig. 5a). The $\delta^{18}O^i_W$ values of magmatic water theoretically inverted from the gneissic country rock, however, are steadily decreased with variation of metamorphic temperatures for sample 01TZS05 (Fig. 5b). Nevertheless, the variability of $\delta^{18}O^i_W$ values is generally less than 0.28 ‰ along with the magmatic or metamorphic temperatures which varied for every 100°C. As the magmatic or metamorphic temperatures are well and tightly constrained (see Table 2 footnote), those temperatures adopted in this study cannot greatly influence the $\delta^{18}O^i_W$ values theoretically inverted (Figs 5a, b) and their reliability is thus guaranteed.

Because of the susceptibility of rock-forming minerals (in particular feldspar) to subsequent water disturbance, the apparent temperature could be yielded in some cases. Adjusting the observed alkali feldspar and quartz $\delta^{18}O$ values to high or low ones, hypothetical temperatures can be accordingly calculated. It can be seen that a large range of $\delta^{18}O^i_W$ values are theoretically inverted with hypothetical temperatures (labelled dashed curves in Figs 5c, d). A cross point, however, occurs for samples 01HP05 and 01TZS05. This means that both quartz and alkali feldspar oxygen isotopes were thermodynamically re-equilibrated with unique meteoric or magmatic water at the same temperature for each sample, which corresponded to the $\delta^{18}O^i_W$ values theoretically inverted with the observed alkali feldspar and quartz $\delta^{18}O$ values (Table 2). In this regard, it suggests that true re-equilibration temperatures are retained and obtained for the studied samples and the $\delta^{18}O^i_W$ values are therefore validated.

7. Kinetic considerations of oxygen exchange

As listed in Tables 2 and 3, the re-equilibration temperatures of the external infiltration of meteoric and magmatic water with rocks are overall less than 350°C. While the susceptible alkali feldspar from the gneissic country rock could re-equilibrate with the externally infiltrated hot magmatic water, an unreasonable timescale up to 450 Myr was required for quartz to diffusively exchange oxygen with water (arrowed line in supplementary Fig. 2). Given that re-equilibrations were achieved and/or reproduced between quartz and alkali feldspar oxygen isotopes for the studied samples (labelled data points in Figs 3–5), this probably suggests that surface reaction instead of volume diffusion actually controlled oxygen exchange during the post-magmatic stage and/or exhumed process of the retrograde metamorphism. Mechanisms such as dissolution, reprecipitation and exchange along micro-fractures and/or within networks were proposed to account for the variations of quartz and/or alkali

https://doi.org/10.1017/S1755691021000244 Published online by Cambridge University Press

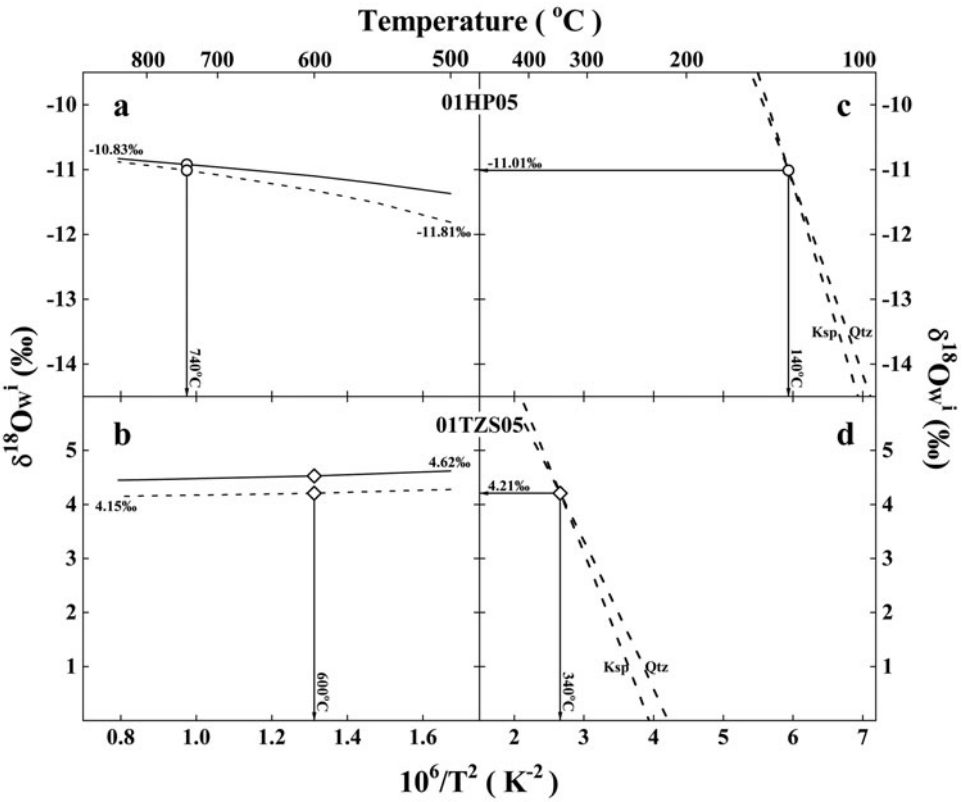

Figure 5 The relationship between temperature and $\delta^{18}O^{i}_{W}$ value of externally infiltrated water theoretically inverted from Dabie orogen in central-eastern China. Parameters refer to Table 2. Labelled solid and dashed curves in (a) and (b) denote $\delta^{18}O^{i}_{W}$ values theoretically inverted for closed and open systems, respectively, along with magmatic or metamorphic temperatures varying from 500 to 850°C. The dependence of the $\delta^{18}O^{i}_{W}$ value on re-equilibration temperature is illustrated in (c) and (d). Dashed curves are theoretically inverted with adjustment of quartz and alkali feldspar $\delta^{18}O$ values to high or low ones for open systems. For other details see the text.

Table 2 Parameters of inversion for the external water infiltration with rock-forming minerals

Sample number	$\delta^{18}O^{i}_{Qtz}$ (‰)	$\delta^{18}O^{i}_{Ksp}$ (‰)	T (°C)	$\delta^{18}O^{i}_{W}$ (‰)
Granitoid				
01HP05	7.74[1]	6.72[1]	140[2]	−11.01[3]
Gneiss				
01TZS05	4.35[4]	3.05[4]	340[2]	4.21[3]
$n^{O}_{Water}/n^{O}_{Mineral}$[5]	1.68	1.93	/	/

[1]Calculated with the observed zircon $\delta^{18}O$ value at 740°C, which is retrieved from the quartz-zircon pair of sample 01HP04 and assumed a similar Teq value on the pluton scale.
[2]Re-equilibration temperature calculated with the observed $\delta^{18}O$ values of the quartz–alkali feldspar pair.
[3]Theoretically inverted with the observed $\delta^{18}O$ values of quartz and alkali feldspar at corresponding re-equilibration temperature for an open system.
[4]Calculated with observed zircon $\delta^{18}O$ values at 600°C, which are retrieved from quartz–zircon pairs of samples 00DB63, 00DB64 and 01TZS07 and assumed a common thermal regime on the regional scale for gneissic country rocks.
[5]Ratio of exchangeable oxygen content between water (89 % oxygen within H_2O molecule) and mineral (53 % oxygen within SiO_2 and 46 % oxygen within $KAlSi_3O_8$ molecules, respectively).

feldspar $\delta^{18}O$ values in the course of hydrothermal alterations (Cole *et al.* 1983, 1992; Matthews *et al.* 1983; Valley & Graham 1996; King *et al.* 1997).

Based on parameters listed in Table 3, the time required to achieve 99 % oxygen exchange between mineral and water is calculated. As the original formulation was proposed for a closed system (Cole *et al.* 1983), the $(W/R)_c$ ratios are thus adopted in this study.

Owing to the slightly high re-equilibration temperature, a maximum timespan of about 12 Kyr is quantified for gneissic country rock externally infiltrated by hot magmatic water from the Tianzhushan granitoid pluton (italic bold number with underline in Table 3). An upper limit duration of *ca.*0.7 Myr, however, is constrained for the granitoid from the Hepeng pluton to achieve re-equilibration between quartz and alkali feldspar oxygen isotopes with externally infiltrated cold meteoric water. Compared with the short-lived magmatic hydrothermal system driven by the small Tianzhushan plutonism, the longer lifetime of the meteoric hydrothermal system could be sustained by the energetic budget of the Hepeng granitoid pluton of moderate size (Fig. 1).

8. Conclusions

Both forward and inverse modellings are conducted to constrain externally infiltrated fossil hydrothermal systems with oxygen isotopes in this study. Only the upper limit of $\delta^{18}O^{i}_{W}$ values and lower limit of re-equilibration temperatures, however, can be loosely estimated by forward modelling for the meteoric hydrothermal system. In contrast, the $\delta^{18}O^{i}_{W}$ values of externally infiltrated meteoric and magmatic water are uniquely inverted with oxygen isotopes of the re-equilibrated rock-forming minerals from the early Cretaceous post-collisional granitoid and intruded Triassic gneissic country rock across the Dabie orogen in central-eastern China, and their reliability is accordingly validated.

A granitoid externally infiltrated by meteoric water with a low $\delta^{18}O^{i}_{W}$ value of −11.01 ‰ is theoretically inverted at 140°C, and the observed $\delta^{18}O$ values of rock-forming minerals were thermodynamically re-equilibrated each other with a minimum $(W/R)_o$ ratio of 1.10. This meteoric hydrothermal system driven by the early Cretaceous post-collisional magmatism could be kinetically

https://doi.org/10.1017/S1755691021000244 Published online by Cambridge University Press

Table 3 Parameters of surface-reaction oxygen exchange for the infiltration of external water with rock-forming minerals

Sample number	T (°C)[1]	$(W/R)_c$[2]	Quartz					Alkali feldspar				
			Xs[3]	ρ[4] ($g\ cm^{-3}$)	log r[5] (moles $O\ m^{-2}\ s^{-1}$)	a[6] (cm)	t[7] (Kyr)	Xs[3]	ρ[4] ($g\ cm^{-3}$)	log r[5] (moles $O\ m^{-2}\ s^{-1}$)	a[6] (cm)	t[7] (Kyr)
Granitoid				2.66					2.56			
01HP05	140	4.45	0.183		−10.14	0.25	***667.7***	0.183		−8.68	0.25	22.3
						0.05	133.5				0.05	4.5
Gneiss												
01TZS05	340	2.85	0.260		−8.27	0.25	***11.6***	0.260		−7.17	0.25	0.9
						0.05	2.3				0.05	0.2

[1]Re-equilibration temperature from Table 2.
[2]$(W/R)_c$ ratio refers to Fig. 3, supplementary Fig. 1.
[3]Mole fraction of mineral oxygen.
[4]Mineral density from Anthony *et al*. (2021).
[5]Rate constant after Cole *et al*. (1983, 1992).
[6]Grain radius.
[7]Time required to achieve 99 % oxygen exchange between mineral and water.

maintained up to 0.7 Myr. However, magmatic water with a moderately high $\delta^{18}O^{i}_{W}$ value of 4.21 ‰ was externally infiltrated with Triassic gneissic country rock at 340°C with a $(W/R)_o$ ratio of 1.23, and a duration no more than 12 Kyr was required to rapidly re-equilibrate between quartz and alkali feldspar oxygen isotopes for this magmatic hydrothermal system.

Thus, externally infiltrated fossil hydrothermal systems driven by magmatism or metamorphism can be theoretically inverted with oxygen isotopes, and their thermodynamic and kinetic processes can be quantified through the partial re-equilibration of constituent minerals. This study can also be applied beyond the Dabie orogen and strengthen our insights for late fluid evolution and thermal history of continental orogens from qualitative inference to quantitative inversion.

9. Acknowledgements

Yong-Fei Zheng is thanked for initiating this study. John W. Valley and Michael J. Spicuzza are acknowledged for hosting and assisting analytical aspects of this work during the senior author's sabbatical visit. This study was funded by the National Natural Science Foundation of China (40173008, 40033010 and 41888101), the Chinese Academy of Sciences (KZCX2-107 and XDB41000000) and the China Scholarship Council of Ministry of Education (20G05006). Thanks are due to two anonymous reviewers for their constructive comments; Chris Soulsby and Susie Cox are appreciated for their editorial handling; the senior author is responsible for any errors if present.

10. Supplementary material

Supplementary material is available online at https://doi.org/10.1017/S1755691021000244

11. References

Ames, L., Zhou, G. Z. & Xiong, B. C. 1996. Geochronology and isotopic character of ultrahigh-pressure metamorphism with implications for collision of the Sino-Korean and Yangtze cratons, central China. *Tectonics* **15**, 472–89.

Anthony, J. W., Bideaux, R. A., Bladh, K. W. & Nichols, M. C. 2021. Handbook of Mineralogy, Mineralogical Society of America, Chantilly, VA 20151-1110, USA. http://www.handbookofmineralogy.org.

Bryant, D. L., Ayers, J. C., Gao, S., Miller, C. F. & Zhang, H. F. 2004. Geochemical, age, and isotopic constraints on the location of the Sino-Korean/Yangtze Suture and evolution of the Northern Dabie Complex, east central China. *Geological Society of America Bulletin* **116**, 698–717.

Cheng, H., Zhang, C., Vervoort, J. D., Wu, Y. B., Zheng, Y. F., Zheng, S. & Zhou, Z. Y. 2011. New Lu-Hf geochronology constrains the onset of continental subduction in the Dabie orogen. *Lithos* **121**, 41–54.

Cole, D. R., Ohmoto, H. & Jacobs, G. K. 1992. Isotopic exchange in mineral-fluid systems: III. Rates and mechanisms of oxygen isotope exchange in the system granite-$H_2O \pm NaCl \pm KC1$ at hydrothermal conditions. *Geochimica et Cosmochimica Acta* **56**, 445–66.

Cole, D. R., Ohmoto, H. & Lasaga, A. C. 1983. Isotopic exchange in mineral-fluid systems. I. Theoretical evaluation of oxygen isotopic exchange accompanying surface reactions and diffusion. *Geochimica et Cosmochimica Acta* **47**, 1681–93.

Criss, R. E. & Taylor, H. P. Jr. 1986. Meteoric-hydrothermal systems. *Reviews in Mineralogy* **16**, 373–424.

Dai, L. Q., Zhao, Z. F. & Zheng, Y. F. 2015. Tectonic development from oceanic subduction to continental collision: geochemical evidence from postcollisional mafic rocks in the Hong'an-Dabie orogens. *Gondwana Research* **27**, 1236–54.

Deng, X., Yang, K. G., Polat, A., Kusky, T. M. & Wu, K. B. 2014. Zircon U-Pb ages, major and trace elements, and Hf isotope characteristics of the Tiantangzhai granites in the North Dabie orogen, Central China: tectonic implications. *Geological Magazine* **151**, 916–37.

Ernst, W. G., Tsujimori, T., Zhang, R. Y. & Liou, J. G. 2007. Permo-Triassic collision, subduction-zone metamorphism, and tectonic exhumation along the East Asian continental margin. *Annual Review in Earth and Planetary Sciences* **35**, 73–110.

Fortier, S. M. & Giletti, B. J. 1989. An empirical model for predicting diffusion coefficients in silicate minerals. *Science (New York, N.Y.)* **245**, 1481–84.

Fu, B., Kita, N. T., Wilde, S. A., Liu, X. C., Cliff, J. & Greig, A. 2013. Origin of the Tongbai-Dabie-Sulu Neoproterozoic low-$\delta^{18}O$ igneous province, east-central China. *Contributions to Mineralogy and Petrology* **165**, 641–62.

Giletti, B. J., Semet, M. P. & Yund, R. A. 1978. Studies in diffusion – III. Oxygen in feldspars: an ion microprobe determination. *Geochimica et Cosmochimica Acta* **42**, 45–57.

Giletti, B. J. & Yund, R. A. 1984. Oxygen diffusion in quartz. *Journal of Geophysical Research* **89**, 4039–46.

Hacker, B. R., Ratschbacher, L., Webb, L., Ireland, T., Walker, D. & Dong, S. W. 1998. U/Pb zircon ages constrain the architecture of the ultrahigh-pressure Qinling-Dabie orogen, China. *Earth and Planetary Science Letters* **161**, 215–30.

Hacker, B. R., Ratschbacher, L., Webb, L., McWilliams, M. O., Ireland, T., Calvert, A., Dong, S. W., Wenk, H. R. & Chateigner, D. 2000. Exhumation of ultrahigh-pressure continental crust in east central China: Late Triassic-Early Jurassic tectonic unroofing. *Journal of Geophysical Research* **105**, 13339–64.

He, Y. S., Li, S. G., Hoefs, J. & Kleinhanns, I. C. 2013. Sr-Nd-Pb isotopic compositions of Early Cretaceous granitoids from the Dabie orogen: constraints on the recycled lower continental crust. *Lithos* **156–159**, 204–17.

Hellmann, R. & Wood, S. A. 2002. Water-rock interactions, ore deposits, and environmental geochemistry: A tribute to David A. Crerar. *Geochemical Society Special Publication* **7**, 1–462.

Henley, R. W., Truesdell, A. H., Barton, P. B. Jr. & Whitney, J. A. 1984. Fluid-mineral equilibria in hydrothermal systems. *Reviews in Economic Geology* **1**, 1–267.

Hochella, M. F. Jr. & White, A. F. 1990. Mineral-water interface geochemistry. *Reviews in Mineralogy* **23**, 1–603.

Holk, G. J., Taylor, H. P. Jr. & Gromet, L. P. 2006. Stable isotope evidence for large-scale infiltration of metamorphic fluids generated during shallow subduction into the Eastern Peninsular Ranges Mylonite Zone (EPRMZ), Southern California. *International Geology Review* **48**, 209–22.

Holk, G. J. & Taylor, H. P. Jr. 2007. $^{18}O/^{16}O$ evidence for contrasting hydrothermal regimes involving magmatic and meteoric-hydrothermal waters at the Valhalla metamorphic core complex, British Columbia. *Economic Geology* **102**, 1063–78.

Holt, E. W. & Taylor, H. P. Jr. 1998. $^{18}O/^{16}O$ mapping and hydrogeology of a short-lived ($\approx$10 years) fumarolic (> 500°C) meteoric-hydrothermal event in the upper part of the 0.76 Ma Bishop Tuff outflow sheet, California. *Journal of Volcanology and Geothermal Research* **83**, 115–39.

Jahn, B.-M., Conichet, J., Cong, B. L. & Yui, T. F. 1996. Ultrahigh-ε_{Nd} eclogites from an ultrahigh-pressure metamorphic terrane of China. *Chemical Geology* **127**, 61–79.

Jahn, B.-M., Wu, F. Y., Lo, C. H. & Tsai, C. H. 1999. Crustal-mantle interaction induced by deep subduction of the continental crust: geochemical and Sr-Nd isotopic evidence from post-collisional mafic-ultramafic intrusions of the northern Dabie complex, central China. *Chemical Geology* **157**, 119–46.

King, E. M., Barrie, C. T. & Valley, J. W. 1997. Hydrothermal alteration of oxygen isotope ratios in quartz phenocrysts, Kidd Creek mine, Ontario: magmatic values are preserved in zircon. *Geology* **25**, 1079–82.

Li, S. G., Jagoutz, E., Chen, Y. Z. & Li, Q. L. 2000. Sm-Nd and Rb-Sr isotopic chronology and cooling history of ultrahigh pressure metamorphic rocks and their country rocks at Shuanghe in the Dabie Mountains, Central China. *Geochimica et Cosmochimica Acta* **64**, 1077–93.

Li, S. G., Xiao, Y. L., Liu, D. L., Chen, Y. Z., Ge, N. J., Zhang, Z. Q., Sun, S.-S., Cong, B. L., Zhang, R. Y., Hart, S. R. & Wang, S. S. 1993. Collision of the North China and Yangtze Blocks and formation of coesite-bearing eclogites: timing and processes. *Chemical Geology* **109**, 89–111.

Liu, D. Y., Jian, P., Kroner, A. & Xu, S. T. 2006. Dating of prograde metamorphic events deciphered from episodic zircon growth in rocks of the Dabie-Sulu UHP complex, China. *Earth and Planetary Science Letters* **250**, 650–66.

Ma, C. Q., Li, Z. C., Ehlers, C., Yang, K. G. & Wang, R. J. 1998. A post-collisional magmatic plumbing system: Mesozoic granitoid plutons from the Dabieshan high-pressure and ultrahigh-pressure metamorphic zone, east-central China. *Lithos* **45**, 431–56.

Matthews, A., Goldsmith, J. R. & Clayton, R. N. 1983. On the mechanisms and kinetics of oxygen isotope exchange in quartz and feldspars at elevated temperatures and pressures. *Geological Society of America Bulletin* **94**, 396–412.

Nabelek, P. I., Labotka, T. C., O'Neil, J. R. & Papike, J. J. 1984. Contrasting fluid/rock interaction between the Notch Peak granitic intrusion and argillites and limestones in western Utah: evidence from stable isotopes and phase assemblages. *Contributions to Mineralogy and Petrology* **86**, 25–34.

Oelkers, E. H. & Schott, J. 2009. Thermodynamics and kinetics of water-rock interaction. *Reviews in Mineralogy and Geochemistry* **70**, 1–569.

Rowley, D. B., Xue, F., Tucker, R. D., Peng, Z. X., Baker, J. & Davis, A. 1997. Ages of ultrahigh pressure metamorphism and protolith orthogneisses from the Central Dabie Shan: U/Pb zircon geochronology. *Earth and Planetary Science Letters* **155**, 191–203.

Rumble, D., Giorgis, D., Oreland, T., Zhang, Z. M., Xu, H. F., Yui, T. F., Yang, J. S., Xu, Z. Q. & Liou, J. G. 2002. Low $\delta^{18}O$ zircons, U-Pb dating, and the age of the Qinglongshan oxygen and hydrogen isotope anomaly near Donghai in Jiangsu province, China. *Geochimica et Cosmochimica Acta* **66**, 2299–306.

Sheppard, S. M. F. 1981. Stable isotope geochemistry of fluids. *Physics and Chemistry of the Earth* **13–14**, 419–45.

Sheppard, S. M. F. 1986. Characterization and isotopic variations in natural waters. *Reviews in Mineralogy* **16**, 165–83.

Spencer, R. J. & Chou, I.-M. 1990. Fluid-mineral interactions: A tribute to H. P. Eugster. *Geochemical Society Special Publication* **2**, 1–432.

Spicuzza, M. J., Valley, J. W. & McConnell, V. S. 1998. Oxygen isotope analysis of whole rock via laser fluorination: an air lock approach. *Geological Society of America Abstracts with Programs* **30**, A80.

Taylor, B. E. & O'Neil, J. R. 1977. Stable isotope studies of metasomatic Ca-Fe-Al-Si skarns and associated metamorphic and igneous rocks, Osgood mountains, Nevada. *Contributions to Mineralogy and Petrology* **63**, 1–49.

Taylor, H. P. Jr. 1971. Oxygen isotope evidence for large-scale interaction between meteoric ground waters and Tertiary granodiorite intrusions, Western Cascade Range, Oregon. *Journal of Geophysical Research* **76**, 7855–74.

Taylor, H. P. Jr. 1977. Water/rock interactions and the origin of H_2O in granitic batholiths. *Journal of Geological Society of London* **133**, 509–58.

Taylor, H. P. Jr., O'Neil, J. R. & Kaplan, I. R. 1991. Stable isotope geochemistry: A tribute to Samuel Epstein. *Geochemical Society Special Publication* **3**, 1–516.

Taylor, H. P. Jr. & Forester, R. W. 1979. An oxygen and hydrogen isotope study of the Skaergaard intrusion and its country rocks: a description of a 55 m.y. old fossil hydrothermal system. *Journal of Petrology* **20**, 355–419.

Turi, B. & Taylor, H. P. Jr. 1971. O^{18}/O^{16} ratios of the Johnny Lyon granodiorite and Texas Canyon quartz monzonite plutons, Arizona, and their contact aureoles. *Contributions to Mineralogy and Petrology* **32**, 138–46.

Valley, J. W. 2003. Oxygen isotopes in zircon. *Reviews in Mineralogy and Geochemistry* **53**, 343–85.

Valley, J. W., Kinny, P. D., Schulze, D. J. & Spicuzza, M. J. 1998. Zircon megacrysts from kimberlite: oxygen isotope variability among mantle melts. *Contributions to Mineralogy and Petrology* **133**, 1–11.

Valley, J. W., Kitchen, N. E., Kohn, M. J., Niendorf, C. R. & Spicuzza, M. J. 1995. UWG-2, A garnet standard for oxygen isotope ratio: strategies for high precision and accuracy with laser heating. *Geochimica et Cosmochimica Acta* **59**, 5223–31.

Valley, J. W., Taylor, H. P. Jr. & O'Neil, J. R. 1986. Stable isotopes in high temperature geological processes. *Reviews in Mineralogy* **16**, 1–570.

Valley, J. W. & Graham, C. M. 1996. Ion microprobe analysis of oxygen isotope ratios in quartz from Skye granite: healed micro-cracks, fluid flow, and hydrothermal exchange. *Contributions to Mineralogy and Petrology* **124**, 225–34.

Valley, J. W. & Cole, D. R. 2001. Stable Isotopes Geochemistry. *Reviews in Mineralogy and Geochemistry* **43**, 1–662.

Walther, J. V. & Wood, B. J. 1986. *Fluid-Rock interactions during metamorphism*. Springer-Verlag, New York, Berlin, Heidelberg, Tokyo, 1–218.

Wang, Q., Wyman, D. A., Xu, J. F., Jian, P., Zhao, Z. H., Li, C. F., Xu, W. X., Ma, J. L. & He, B. 2007. Early Cretaceous adakitic granites in the Northern Dabie Complex, central China: implications for partial melting and delamination of thickened lower crust. *Geochimica et Cosmochimica Acta* **71**, 2609–36.

Wang, X. M., Liou, J. G. & Mao, H. K. 1989. Coesite-bearing eclogite from the Dabie Mountains in central China. *Geology* **17**, 1085–88.

Watson, E. B. & Cherniak, D. J. 1997. Oxygen diffusion in zircon. *Earth and Planetary Science Letters* **148**, 527–44.

Wei, C. S., Zhao, Z. F. & Spicuzza, M. J. 2008. Zircon oxygen isotopic constraint on the sources of late Mesozoic A-type granites in eastern China. *Chemical Geology* **250**, 1–15.

Wei, C. S. & Zhao, Z. F. 2017. Dual sources of water overprinting on the low zircon $\delta^{18}O$ metamorphic country rocks: disequilibrium constrained through inverse modelling of partial reequilibration. *Scientific Reports* **7**, 40334.

Wickham, S. M., Peters, M. T., Fricke, H. C. & O'Neil, J. R. 1993. Identification of magmatic and meteoric fluid sources and upward- and downward-moving infiltration fronts in a metamorphic core complex. *Geology* **21**, 81–4.

Wickham, S. M. & Taylor, H. P. Jr. 1985. Stable isotopic evidence for large-scale seawater infiltration in a regional metamorphic terrane; the Trois Seigneurs Massif, Pyrenees, France. *Contributions to Mineralogy and Petrology* **91**, 122–37.

Wickham, S. M. & Taylor, H. P. Jr. 1987. Stable isotope constraints on the origin and depth of penetration of hydrothermal fluids associated with Hercynian regional metamorphism and crustal anatexis in the Pyrenees. *Contributions to Mineralogy and Petrology* **95**, 255–68.

Xu, H. J., Ma, C. Q., Zhang, J. F. & Ye, K. 2012. Early Cretaceous low-Mg adakitic granites from the Dabie orogen, eastern China: petrogenesis and implications for destruction of the over-thickened lower continental crust. *Gondwana Research* **23**, 190–207.

Xu, S. T., Okay, A. I., Ji, S. Y., Sengor, A. M. C., Su, W., Liu, Y. C. & Jiang, L. L. 1992. Diamond from the Dabie Shan metamorphic rocks and its implication for tectonic setting. *Science (New York, N.Y.)* **256**, 80–2.

Xu, X. J., Zhao, Z. F., Zheng, Y. F. & Wei, C. S. 2005. Element and isotope geochemistry of Mesozoic intermediate-felsic rocks at Tianzhushan in the Dabie orogen. *Acta Petrologica Sinica* **21**, 607–22.

Xue, F., Rowley, D. B., Tucker, R. D. & Peng, Z. X. 1997. U-Pb zircon ages of granitoid rocks in the north Dabie complex, eastern Dabie Shan, China. *Journal of Geology* **105**, 744–53.

Ye, K., Cong, B. L. & Ye, D. N. 2000. The possible subduction of continental material to depths greater than 200 km. *Nature* **407**, 734–36.

Zhang, H. F., Gao, S., Zhong, Z. Q., Zhang, B. R., Zhang, L. & Hu, S. H. 2002. Geochemical and Sr-Nd-Pb isotopic compositions of Cretaceous granitoids: constraints on tectonic framework and crustal structure of the Dabieshan ultrahigh-pressure metamorphic belt, China. *Chemical Geology* **186**, 281–99.

Zhao, Z. F., Zheng, Y. F., Wei, C. S., Chen, F. K., Liu, X. M. & Wu, F. Y. 2008. Zircon U-Pb ages, Hf and O isotopes constrain the crustal architecture of the ultrahigh-pressure Dabie orogen in China. *Chemical Geology* **253**, 222–42.

Zhao, Z. F., Zheng, Y. F., Wei, C. S. & Wu, F. Y. 2011. Origin of postcollisional magmatic rocks in the Dabie orogen: implications for crust-mantle interaction and crustal architecture. *Lithos* **126**, 99–114.

Zhao, Z. F., Zheng, Y. F., Wei, C. S. & Wu, Y. B. 2004. Zircon isotope evidence for recycling of subducted continental crust in post-collisional granitoids from the Dabie terrane in China. *Geophysical Research Letters* **31**, L22602.

Zhao, Z. F., Zheng, Y. F., Wei, C. S. & Wu, Y. B. 2007. Post-collisional granitoids from the Dabie orogen in China: Zircon U-Pb age, element and O isotope evidence for recycling of subducted continental crust. *Lithos* **93**, 248–72.

Zhao, Z. F., Zheng, Y. F., Wei, C. S., Wu, Y. B., Chen, F. K. & Jahn, B.-M. 2005. Zircon U-Pb age, element and C-O isotope geochemistry of post-collisional mafic-ultramafic rocks from the Dabie orogen in east-central China. *Lithos* **83**, 1–28.

Zheng, Y. F. 1993. Calculation of oxygen isotope fractionation in anhydrous silicate minerals. *Geochimica et Cosmochimica Acta* **57**, 1079–91.

Zheng, Y. F. 2012. Metamorphic chemical geodynamics in continental subduction zones. *Chemical Geology* **328**, 5–48.

Zheng, Y. F., Fu, B., Gong, B. & Li, L. 2003. Stable isotope geochemistry of ultrahigh pressure metamorphic rocks from the Dabie-Sulu Orogen in China: implications for geodynamics and fluid regime. *Earth-Science Reviews* **62**, 105–61.

Zheng, Y. F., Wu, Y. B., Chen, F. K., Gong, B., Li, L. & Zhao, Z. F. 2004. Zircon U-Pb and oxygen isotope evidence for a large-scale ^{18}O depletion event in igneous rocks during the Neoproterozoic. *Geochimica et Cosmochimica Acta* **68**, 4145–65.

Zheng, Y. F. & Fu, B. 1998. Estimation of oxygen diffusivity from anion porosity in minerals. *Geochemical Journal* **32**, 71–89.

MS received 28 June 2020. Accepted for publication 27 May 2021. First published online 30 June 2021